MINIATURE OPTICAL WIDE-ANGLE-LENS STARTRACKER (MINI-OWLS)

Major Rick Miller, Wright Laboratory,
WL/MNSI, Eglin AFB, Florida

Joe E. Coulter and Seymour Levine
Northrop Corporation, Electronics Systems Division,
Hawthorne, California

ABSTRACT

This paper provides a brief overview of the design considerations and the current status of the Miniature Optical Wide-Angle Lens Startracker program. Mini-OWLS offers a revolutionary alternative to the conventional startracker. It is a small, lightweight, low-cost, high performance startracker that can be used in a variety of applications including calibration and alignment of Inertial Measurement Units (IMUs).

Mini-OWLS makes use of a strapdown design incorporating Holographic Optical Elements (HOEs) in place of conventional optics. HOEs can be multiplexed so that the same aperture can be used for multiple separate optical paths looking in several directions simultaneously without startracker rotation. Additionally, separate Schmidt corrector plates are not required to compensate for spherical aberration. The optical assembly, or what would normally be considered as the telescope, is less than 20 cm^3 in volume, weighs less than 55 grams, and contains the equivalent of three individual telescopes. Each one has a 4 deg Field of View (FOV) with a field of regard of 48 square degrees. Mini-OWLS has a bandwidth of approximately 300 nm in or near the visible wavelength. The projected resolution of the startracker is 5 to 10 arc-seconds, depending on the centroiding algorithm used.

The Mini-OWLS program was initiated last year and represents a miniaturized version of a similar design for aeronautical applications. The contract is managed by Wright Laboratory, Air Force Systems Command, Wright-Patterson AFB, Ohio, with funding from the Strategic Defense Initiative Organization through Eglin AFB. The initial phase of the program is to build and test a development unit. The second phase is to integrate the startracker with the Charles Stark Draper Laboratory Micromechanical Inertial Guidance System (MIGS) and the Signal Processing Packaging Design (SPPD) being developed by Texas Instruments. The preliminary design review was conducted in November 1991. Three-axes prototype telescope assemblies have been built and design evaluation tests initiated.

INTRODUCTION

Stellar trackers can provide the fiducial reference for attitude control systems for air vehicles, satellites, and space-based interceptors. The independence of stellar fixes from radio aids has provided a reliable source of navigation information in both peace and war. When the stellar tracker is used to augment an IMU, a synergistic blending of data occurs where the high-frequency attitude data is derived from the IMU, and the low-frequency information is derived from stellar fixes. This process of complementary filtering of data provides excellent attitude information that is accurate over a wide range of frequencies. Furthermore, since the low frequency is derived from the stellar tracker, the requirement for precision and costly gyroscopes for attitude control has been reduced.

Figure 1 shows the probability of seeing the sky from sea level. Above 13.7 km (45,000 ft) in altitude, the probability of having an unobstructed view of the stars is essentially 100 percent. Although at an altitude of 13.7 km your view of the sky is unobstructed by cloud coverage, the sky background light will prevent you from observing the stars in the daylight. Yet at night, the view of the stars, from that altitude, is spectacular. Above 13.7 km, the daytime sky background, not in the direct vicinity of the sun, grows progressively darker with increases in altitude until it essentially turns black and is indistinguishable from the nighttime sky. Figure 2 shows the star magnitude capability versus altitude for two different-aperture telescopes in daylight. Basically, it shows that observing stars in daylight at sea level with a 232 cm^2 (36 in^2) aperture, 3 deg FOV telescope has essentially the same stellar magnitude capability as a 4.65 cm^2 (0.72 in^2) aperture operating at 97 km (60 mi) above the earth. It also shows that at altitudes above 97 km, there is no improvement in star magnitude capability, for a given telescope, since the sky background noise has reached a minimum and the stellar irradiance experiences no loss due to atmospheric transmission. Table 1 is a simplistic Signal-to-Noise Ratio (SNR) equation definition for stellar trackers. The small-aperture telescope is in good correlation with our experience on a clear, moonless, desert night. Under these conditions an observer can easily see the Little Dipper constellation, which has 4.7 magnitude stars. In fact, under good stellar observation conditions, the human eye can detect magnitude 6 stars at sea level. The eye has a pupil diameter of between 6 and 9 mm, corresponds to an aperture of about 0.6 cm^2, and is

much smaller than the 4.6 cm^2 telescope in the star magnitude capability curve of Figure 2.

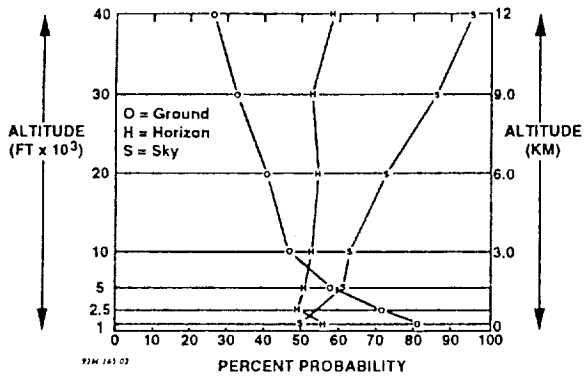

Figure 1. Probability of Clear Lines of Sight Over the Northern Hemisphere for All Seasons Combined (72,000 Observations)

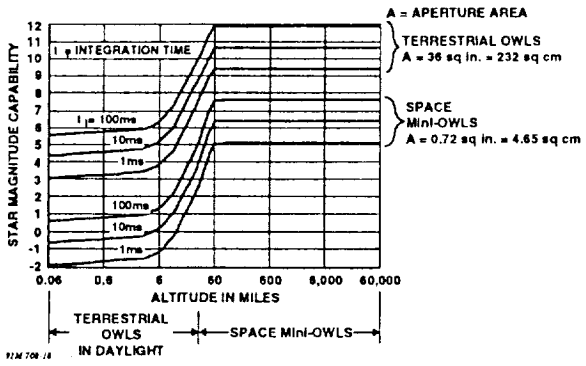

Figure 2. Star Tracker Sensed Magnitude Versus Altitude for a Silicon Detector and a 3 Deg FOV

Thus, based on our experience, empirical measurements, and analysis, the SDI Organization in Washington, D.C., Wright Laboratories in Dayton, Ohio, and Eglin AFB, Florida, and Northrop have embarked on the design of a Miniature Optical Wide-Angle Startracker. This telescope is specifically designed to correct the attitude of spaceships, satellites, and space-based interceptors. In this capacity it provides the fiducial reference for the vehicle's attitude control system.

STELLAR TRACKER CONCEPTS

The stellar tracker, unlike an observation telescope, is specifically designed to correct the attitude control system of a vehicle and is therefore primarily concerned with the line of sight (LOS) to the stars. Thus the spectral content and stellar magnitude are of minor significance if they provide sufficient stellar irradiance to satisfy the functional

Table 1. Signal-To-Noise Ratio Equations For a Stellar Tracker

Signal-To-Noise Ratio (SNR)

$$Q_{SP} = q \cdot \Phi_S \cdot \Delta\lambda \cdot A_T \cdot A_a \cdot T_T \cdot \eta \cdot I_t \cdot N_I / N_S$$

Where:

- Q_{SP} = Star signal charges per pixel
- q = Electronic charge
- Φ_S = Stellar spectral radiance
- $\Delta\lambda$ = Wavelength bandwidth of telescope system
- A_T = Atmosphere transmission
- A_a = Aperture area
- T_T = Telescope transmission
- η = Quantum efficiency
- I_t = Integration time of a frame (stellar snapshot)
- N_I = Number of frame snapshots utilized
- N_S = Number of pixels containing the star image (star blur factor)

$$Q_{BP} = \frac{q \cdot \Phi_B \cdot \Delta\lambda \cdot A_a \cdot T_T \cdot FOV \cdot \eta \cdot I_t \cdot N_I}{N \cdot O_F}$$

Where:

- Q_{BP} = Background photo charges per pixel
- Φ_B = Sky background spectral radiance
- FOV = Field of view
- N = Total number of pixels in sensor array
- O_F = Sky background attenuation of optical filter

$$Q_{DP} = q \cdot n i / \tau \cdot V_B \cdot I_t \cdot N_I$$

Where:

- Q_{DP} = Detector dark durrent charges per pixel
- n = Detector intrinsic carrier concentration
- τ = Detector dark current charge generation time
- V_B = Detector charge generation bucket volume

$$Q_{NP} = \sqrt{(Q_{SP} + Q_{BP} + Q_{DP})\, Q_{ES}}$$

Where:

- Q_{NP} = Noise charges per pixel
- Q_{SP} = Star photo charges per pixel
- Q_{BP} = Background photo charges per pixel
- Q_{DP} = Dark detector charges per pixel
- Q_{ES} = Electronic system bandwidth noise coefficient

$$SNR = \frac{Q_{SP}}{\sqrt{(Q_{SP} + Q_{BP} + Q_{DP})\, Q_{ES}}}$$

For Sea-Level Daytime Tracking in a Non-Nuclear-Event Environment, the SNR equation simplifies to:

$$Q_{BP} >> Q_{SP} + Q_{DP}$$

$$SNR \approx \frac{Q_{SP}}{\sqrt{Q_{BP} \cdot Q_{ES}}}$$

$$SNR \approx \frac{\Phi_S \cdot A_T}{N_S} \cdot \sqrt{\frac{q \cdot \Delta\lambda \cdot A_a \cdot T_T \cdot \eta \cdot I_t \cdot N_I \cdot N \cdot O_F}{\Phi B \cdot FOV \cdot Q_{ES}}}$$

92M-165-07

SNR requirements of the tracker. This occurs when there is sufficient stellar photon flux to offset the corrupting noise sources. Figure 3 shows the conceptual design of the Mini-OWLS. It is made up of three 4-deg-FOV star trackers spaced 120 deg apart in azimuth and 30 deg off the zenith, all embedded in a single housing. The star tracker's function is to measure the attitude drift about three orthogonal vehicle axes. A single stellar fix only provides an attitude update about the two vehicle's axes normal to the star's LOS. Thus, in order to provide a complete three-axes attitude update, an additional fix from a different LOS is required. The ideal geometric separation is to have the two LOSs cross each other and thus have an angular separation of 90 deg. This 90-deg separation in the LOSs could be accomplished by mounting a single axis telescope in gimbals and then rotating the gimbals to observe a different LOS. Another method of obtaining different LOSs is to have a strapdown telescope and then rotate the vehicle to observe a different LOS. Both of the above methods of obtaining different LOSs either add costly moving parts to the system or impose constraints on the vehicle. The low-cost Mini-OWLS, with its three implicit strapdown telescopes, requires no gimbals or vehicle rotations to observe multiple LOSs.

When the optimum 90-deg separation isn't achieved, there is a Geometric Dilution of Precision (GDOP). Although the Mini-OWLS has a 51.3-deg separation in telescope axes, its GDOP, as shown in Figure 4, is negligible. This figure also shows that a single 20-deg very wide FOV telescope, or dual telescopes with an angular separation of 20 deg, experiences significant GDOP problems. Furthermore, having three telescopes, each of which provides two axes of attitude updates, enables the system to provide a redundant attitude compensation for all three vehicle axes.

In addition, the redundant telescope design provides a measure of self compensation for thermal mechanical expansion of the stellar tracker. Figure 5 shows a two-axis tracker with stars in each FOV. When the attitude of the vehicle changes about an axis orthogonal to the plane of the telescopes, both telescopes observe identical variations in attitude and direction. Conversely, when the telescope

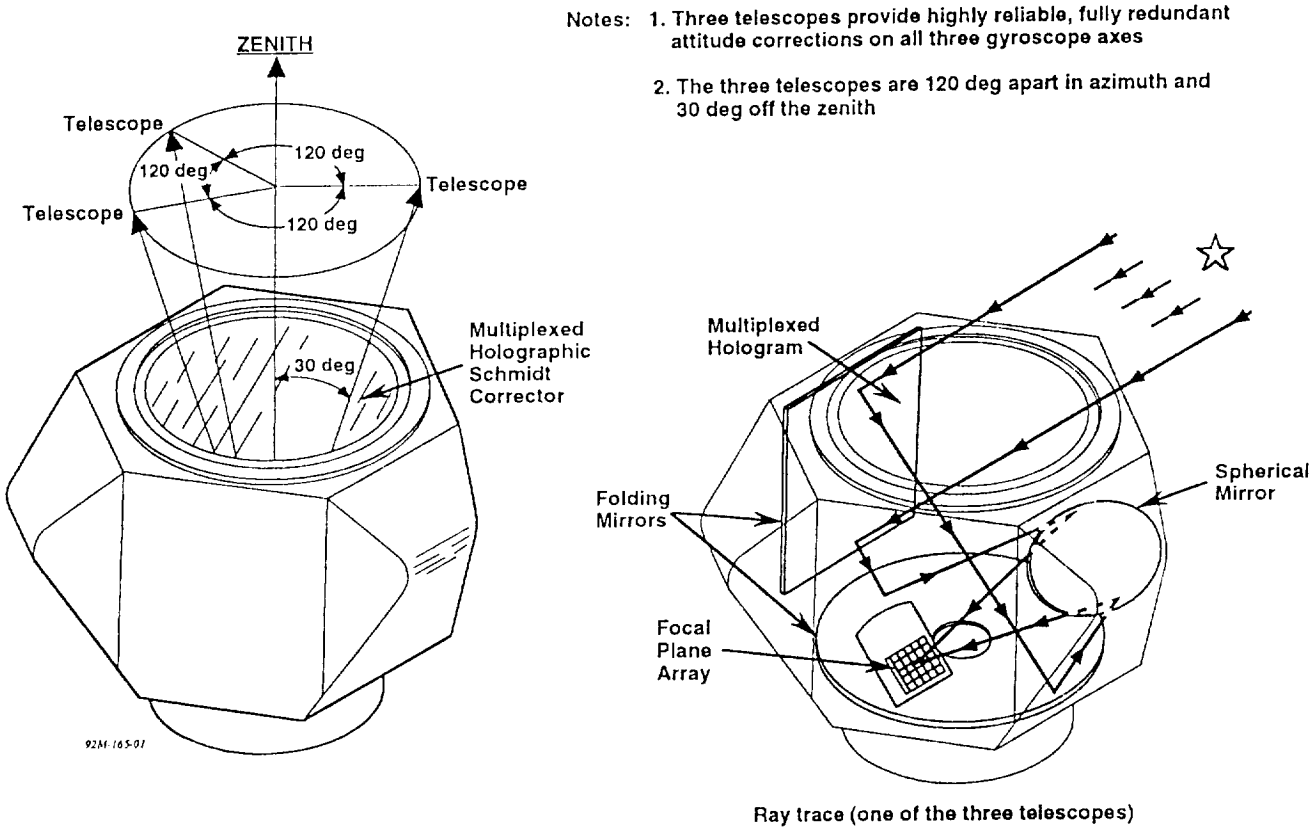

Figure 3. Mini-OWLS Multiplexes Three Wide-Field Schmidt Telescopes in a Single Housing

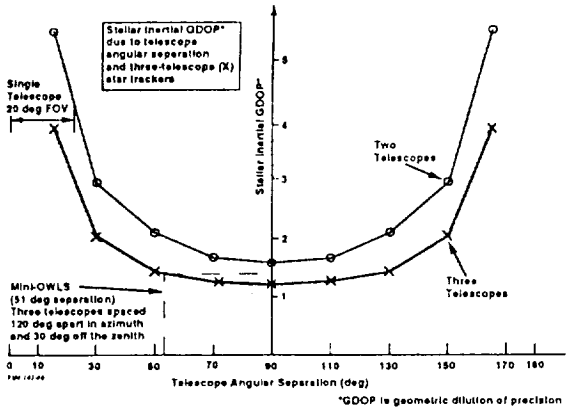

Figure 4. Astro-Inertial GDOP Due to Telescope Angular Separation

structure expands homogeneously, then the attitude variations of the telescopes change equally in magnitude but in opposite directions. Thus the average attitude associated with the expansion of the telescopes is zero.

This self-compensation feature is optimized in the Mini-OWLS design since three telescopes represent the minimum number of stellar trackers required to achieve self compensation.

TELESCOPE CONSTRUCTION

Figure 6 shows the spherical aberration of an uncompensated spherical mirror. Its focus occurs at half the mirror's radius for the plane-wave rays close to the principal axis ray. As the height, h, of the plane wave increases from the principal ray axis, the focus decreases slightly from its half-radius focal length, resulting in a blurred focus. This spherical aberration can be minimized by the insertion of an aspheric Schmidt corrector plate positioned at the mirror radius. The aspheric corrector plate attempts to deviate the plane-wave rays such that all plane rays focus at a single point or focal length independent of the height of the plane wave above the principal ray axis.

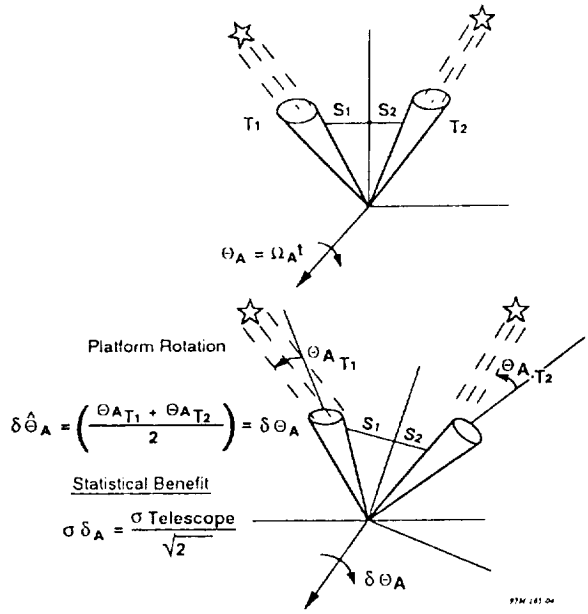

Note 1: For a platform rotation, both telescopes experience the same stellar deviation angle

Figure 5a. Mini-OWLS Provides the Benefit of Redundant Observations

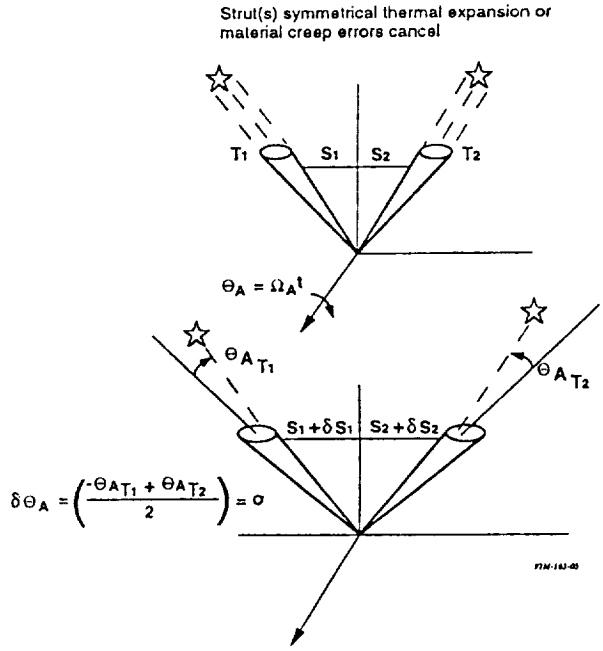

Note 2: For a symmetrical strut with thermal expansion or material creep the average observed stellar deviation is zero. Thus the redundant telescope cancels many thermal expansion errors.

Figure 5b. Mini-OWLS Minimizes Telescope Strut Expansion Errors

Figure 5. Mini-OWLS Provides the Benefit of Redundancy and Self Compensation for Thermal Expansion and Material Creep

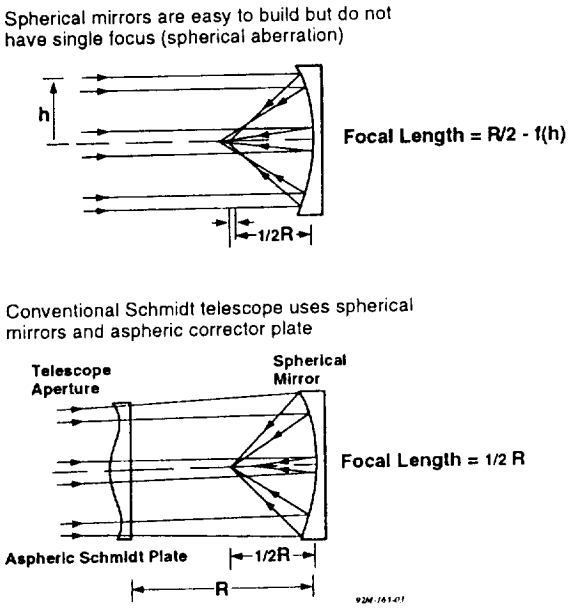

Figure 6. Spherical Aberration

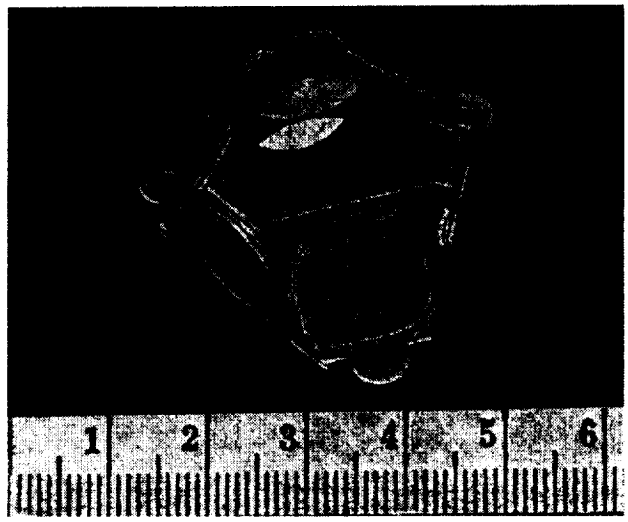

Figure 7. Mini Optical Wide-Angle Lens Startracker (Size in Centimeters)

The aspheric Schmidt corrector plate is costly to make and could be replaced by a single Holographic Optical Element (HOE). Furthermore, three holographic Schmidt corrector plates can be multiplexed in a single aperture. A picture of the Mini-OWLS is shown in Figure 7.

The Mini-OWLS is composed of three wide-FOV Schmidt camera telescopes. The corrector plate for all three telescopes is a multiplexed HOE in lieu of the costly aspheric corrector plates in conventional Schmidt cameras. This unique HOE construction eliminates all costly optical elements since the plane and spherical mirror surfaces are simple to construct. Because all of the optical elements are essentially surface phenomena (i.e., mirrors and HOEs), the telescope can be made extremely lightweight. The telescope construction is based on proven industrial techniques with the single three-axes multiplexed HOE Schmidt corrector plate fastened to the telescope along with the FPAs. The telescope's major precision assemblies are in the mirror housing. The single multiplexed HOE provides the corrector plates for the spherical aberration, while the FPAs provide the electrical readouts of the stellar irradiances.

SUN THERMAL ANALYSIS

Solar heating effects on a silicon FPA in the Mini-Owls star sensor at its operating bandwidth are not important. Under space illumination conditions with the sun focused on four pixels, assuming a constant-temperature mounting surface at any temperature, only a 4.5 °C temperature change will occur.

STRAY LIGHT MEASUREMENTS

Stray light measurements were made using the Mini-OWLS prototype telescope. Figure 8 depicts the experiment setup. With the simulated sun set 30 deg off one telescope axis, the stray light detected in the other two axes as a fraction of the incident beam was negligible. With the simulated sun directly on-axis, the optical crosstalk detected at the FPA for a second telescope was higher, as expected, and is readily reducible to an acceptable level by optimizing the optical surfaces to reduce the scattered light.

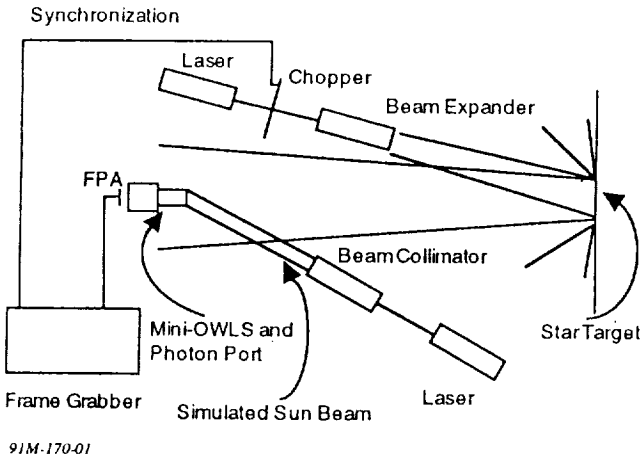

Figure 8. Solar Stray Light Experiment

CONCLUSION

The Mini-OWLS represents a radical departure in star tracker design. It is an optimum configuration that is specifically designed to provide a three-axes fiducial attitude reference system that augments the high-frequency attitude control system for a host of vehicles. The design minimizes weight and telescope expansion errors. It maximizes mission success by providing high accuracy and reliability along with built-in redundancy and self test.